IOP Publishing Measurement Science and Technology

Meas. Sci. Technol. **29** (2018) 075303 (8pp) https://doi.org/10.1088/1361-6501/aac3b5

Calibrationless rotating Lorentz-force flowmeters for low flow rate applications

M G Hvasta, D Dudt, A E Fisher and E Kolemen

Princeton University, Princeton, NJ 08544, United States of America

E-mail: MHvasta@Princeton.edu

Received 28 February 2018, revised 27 April 2018
Accepted for publication 10 May 2018
Published 29 May 2018

Abstract

A 'weighted magnetic bearing' has been developed to improve the performance of rotating Lorentz-force flowmeters (RLFFs). Experiments have shown that the new bearing reduces frictional losses within a double-sided, disc-style RLFF to negligible levels. Operating such an RLFF under 'frictionless' conditions provides two major benefits. First, the steady-state velocity of the RLFF magnets matches the average velocity of the flowing liquid at low flow rates. This enables an RLFF to make accurate volumetric flow measurements without any calibration or prior knowledge of the fluid properties. Second, due to minimized frictional losses, an RLFF is able to measure low flow rates that cannot be detected when conventional, high-friction bearings are used. This paper provides a brief background on RLFFs, gives a detailed description of weighted magnetic bearings, and compares experimental RLFF data to measurements taken with a commercially available flowmeter.

Keywords: low-friction bearings, Lorentz-force velocimetry, flowmeter, liquid metal

(Some figures may appear in colour only in the online journal)

1. Introduction[1]

Shercliff developed the rotating Lorentz-force flowmeter (RLFF) in the 1950s [1–3]. As depicted in figure 1, a double-sided, disc-style RLFF consists of evenly-spaced permanent magnets that are installed near the periphery of a disc or flywheel. The center of the magnet assembly is connected to a low-friction bearing that permits rotational motion. When the flowmeter is installed alongside a pipe or tube that is filled with a flowing, electrically-conductive liquid, the resultant Lorentz-force between the liquid and magnets generates a torque upon the magnet assembly that causes it to rotate. During operation, the average velocity of the liquid can be determined by measuring the corresponding angular velocity of the flowmeter.

RLFFs are inexpensive to manufacture and simple to install. Moreover, RLFFs are non-contact devices that do not introduce any moving parts or seals into piping or tubing networks, so they can safely operate within systems containing chemically aggressive, hazardous, or very high-temperature fluids (e.g. molten metals, strong acids, etc). Collectively, these features make RLFFs useful instruments that could benefit the nuclear, concentrated solar power, chemical, pharmaceutical, and metallurgical/casting industries.

Previous work with RLFFs has shown that a minimum flowrate is required to overcome the static friction or 'stiction' found in conventional bearings [4–6]. Below the minimum flowrate, an RLFF does not spin and velocity measurements are impossible. Depending on the bearings used within an RLFF, the minimum flowrate could be quite large. Above the minimum flow rate, once the RLFF has been set in to motion, frictional forces acting upon the flowmeter must be accounted for in order to accurately correlate the angular velocity of the RLFF to the velocity of the flowing liquid [5, 7].

To avoid this issue, researchers have developed a variety of non-rotating Lorentz force flowmeters that can be used for a wide range of fluids and flow rates [8–11]. However, all of these flowmeters require calibration involving either analytical and/or numerical modeling [12–14], external calibration equipment [15, 16], or redundant flowmeters [4, 17]. This need for calibration introduces inconvenience and added expense that prevents Lorentz-force velocimetry from being more widely adopted in a range of industrial applications.

[1] Parts of this section have been adapted from: M G Hvasta *et al* 2017 *Meas. Sci. Technol.* **28** 085901.

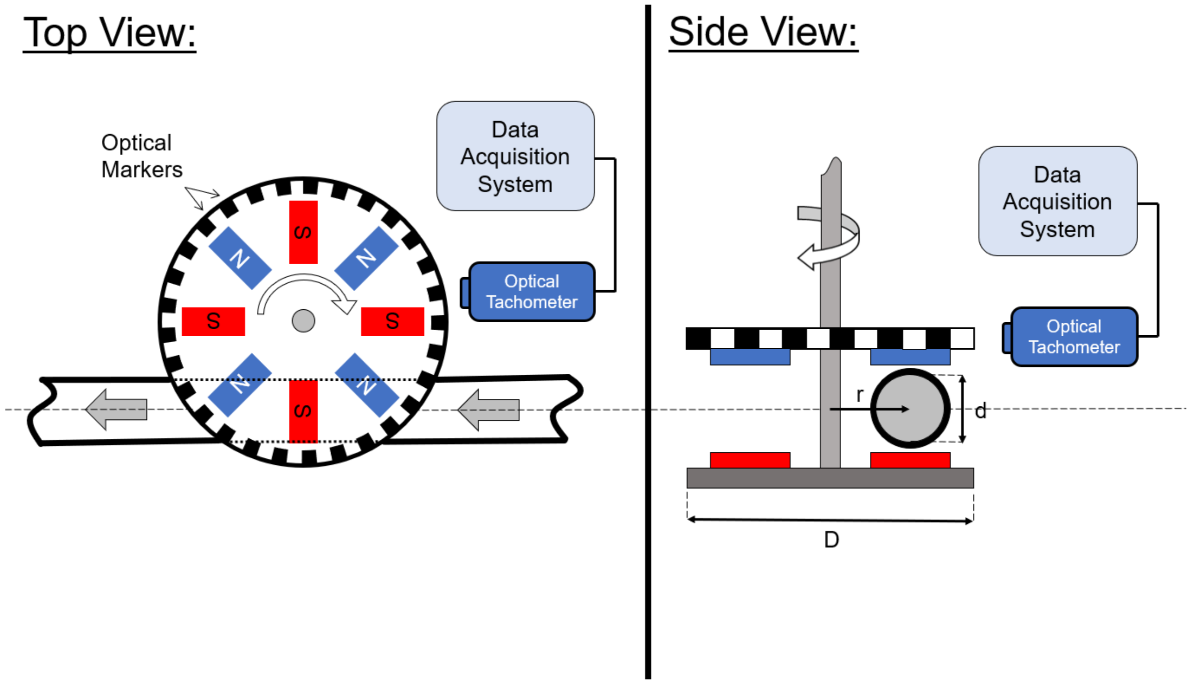

Figure 1. A depiction of a RLFF. In the 'side view', the flow is directed out of the page. Adapted from [5]. © 2017 Not subject to copyright in the USA. Contribution of U.S. Department of Energy.

To address these problems, this paper investigates the use of a new 'weighted magnetic bearing' (WMB) within an RLFF. It was found that the new bearing reduces the impact of friction on RLFF performance to negligible levels. From a practical standpoint, there were two major benefits to operating under 'frictionless' conditions. First, the RLFF was able to measure low flow rates that could not be detected when conventional bearings were used [5]. Second, since the trivially small frictional forces did not meaningfully affect the motion of the RLFF discs, the magnets moved at the average velocity of the flow, as predicted by Bucenieks [18]. This enables an RLFF to make accurate volumetric flow measurements without any calibration or prior knowledge of the fluid properties.

This paper is organized as follows. An overview of RLFF theory is presented in section 2, where attention is focused on the impact of the fluid velocity profile and the RLFF equations of motion. The different loss mechanisms inherent to the RLFF used in this experiment are described in section 3. It is emphasized that frictional losses in the bearing can be minimized while other loss mechanisms, such as windage losses, are only negligibly small at low angular velocities. Accordingly, the RLFF used in this experiment can only be expected to operate without calibration for low flow rates. The experimental setup used to test WMB operation is described in section 4. Experimental results comparing the calibrationless RLFF to a commercially available flowmeter can be found in section 5. The experiments showed that the RLFF flow measurements closely agreed with the commercially available flowmeter. A discussion of the results and a possible path forward for RLFF research is given in section 6.

2. RLFF theory

2.1. Impact of velocity profile

As explained in previous works [4, 15, 19], the Lorentz drag force (F_D) between a flowing, electrically-conductive liquid and the RLFF magnets can typically be described as

$$F_D \propto \sigma \ (v_0 - v_{mag}) \ B^2$$

$$F_D \propto \sigma \ v_{rel} \ B^2 \tag{1}$$

where σ is the electrical conductivity of the fluid, v_0 is the average velocity of the fluid, v_{mag} is the average magnet velocity, B is the magnitude of the externally applied magnetic field, and v_{rel} is the relative velocity between the magnets and the fluid.

There are two notable situations where equation (1) may not yield accurate results. First, for equation (1) to be valid the magnitude of the induced or 'secondary' magnetic field (b) must be negligible compared to the external magnetic ($b \ll B$) [20, 21]. This condition is satisfied if the magnetic Reynolds # (Re_m) is very small. For an RLFF, Re_m can be calculated as

$$\mathrm{Re}_m = \frac{\text{Magnetic Induction}}{\text{Magnetic Diffusion}} = v_{rel} D_h \mu_0 \sigma \tag{2}$$

where D_h is the hydraulic diameter of the flow. It is conceivable that Re_m could become quite large in fast-flowing systems where friction or other loss mechanisms prevent the RLFF magnets from moving at velocities comparable to v_0. Second, equation (1) may not be valid for free-surface applications where large electromagnetic forces could cause fluid 'pile-up' and disrupt flow conditions [16].

However for this work and other similar research projects dealing with electrically conductive flows through pipes or tubes, numerous experiments have demonstrated the validity of equation (1) and verified the implicit assumption that Lorentz-force flowmeters are insensitive to different velocity profiles [5, 12, 18, 22]. In multiple studies, equation (1) has been experimentally confirmed by installing adjustable flow blockages just upstream of Lorentz-force flowmeters and then investigating the changes in the measured output. In these experiments it was found that the Lorentz-force flowmeter measurements were not affected by the changes in the velocity profile, especially at lower flow rates [4, 6, 11, 16]. Similarly, equation (1) has also been validated through experiments where flowing liquid systems were modeled or calibrated using uniform velocity profiles (slug-flow). The accuracy of the 'slug-flow' approximation was demonstrated numerically in turbulent salt-water flows [10] and experimentally in calibration facilities where solid metal proxies are used to calibrate Lorentz-force flowmeters [15]. In general, it is acknowledged that the indifference of Lorentz-force flowmeters towards the peculiarities of a given velocity profile make them useful and versatile for volumetric flow rate measurements [4, 18].

Nonetheless, it is recommended that flowmeter best-practices are followed whenever installing RLFFs (e.g. avoid bubbles/entrained gas, ensure the duct is completely filled, use flow conditioners if required, etc) [23–25]. If operators believe transient or otherwise atypical velocity profiles are a concern during flow measurement, a hydrodynamic entrance length (L) of approximately ten hydraulic diameters has been found to provide a nearly developed velocity profile for many applications [26]. Otherwise, the hydrodynamic entrance length for specific flows can be calculated using correlations below [26, 27]:

$$\begin{aligned} \text{Laminar:} \quad & \frac{L}{D_h} = 0.05\text{Re} = 0.05\left(\frac{\rho v_0 D_h}{\mu}\right) \\ \text{Turbulent:} \quad & \frac{L}{D_h} = 1.359\text{Re}^{0.25} = 1.359\left(\frac{\rho v_0 D_h}{\mu}\right)^{0.25} \end{aligned} \tag{3}$$

where μ and ρ are the viscosity and density of the fluid respectively.

2.2. Flowmeter equations of motion

When an RLFF is used to measure the velocity of an electrically-conductive fluid moving through a duct that is both electrically-insulating and non-magnetic, the total torque on the flowmeter can be described as [5]

$$\sum \tau = \tau_L\left[v_0 - \omega\, r\right] + \tau_F\left[\omega\right] = I\alpha$$

$$\sum \tau = K_L\left(v_0 - \omega\, r\right) + \left(\tau_B\left[\omega\right] + \tau_W[\omega]\right) = I\alpha \tag{4}$$

where τ_L is the torque generated by the Lorentz drag force (F_D), ω is the angular velocity of the RLFF, r is the effective radius of the RLFF, τ_F is the net frictional torque resulting from the combined losses in the bearings (τ_B) and air resistance (τ_W), I is the moment of inertia of the RLFF, and α is the angular acceleration of the RLFF. The constant K_L accounts for the fluid, magnetic, and geometric properties of a particular RLFF setup.

Under idealized conditions, where there are no frictional losses in the flowmeter ($\tau_F = 0$), equation (4) shows that the magnet velocity would match the fluid velocity during steady-state operation ($\alpha = 0$), namely

$$v_0 = \omega\, r. \tag{5}$$

In practice, a real flowmeter will always have some frictional losses, but the goal of this study is to design and build a calibrationless RLFF that minimizes these losses to such an extent that assuming $\tau_F = 0$ leads to acceptably small errors in flow measurements. The next section will describe ways to quantify and minimize forces that oppose the rotation of an RLFF.

3. Bearing and windage losses

3.1. Bearing losses

For this experiment the losses in the bearing can be categorized as either frictional losses (P_F) or eddy current losses (P_{EC}).

3.1.1. Frictional losses. Frictional losses (P_F) in a rotating body can be described using the following equations [28–30]:

$$P_F = \tau_f\, \omega \tag{6}$$

$$\tau_f = \int_0^{r_F} \mu_K[r]\, F_N[r]\, \mathrm{d}r \tag{7}$$

where τ_f is the frictional torque, r_F is the lever-arm associated with the frictional forces, μ_K is the coefficient of kinetic friction, and F_N is normal force between the sliding surfaces within a bearing.

The WMB used in this experiment is depicted in figure 2. The WMB reduces P_F in three ways. First, μ_K is minimized by carefully selecting sliding surfaces to be hard and smooth. The coefficient of kinetic friction is further reduced by lubricating the sliding surfaces. Secondly, the lever-arm that the frictional forces use to act upon the rotating body is minimized by centering the connection between the two spheres directly above the RLFF. In theory the contact area between two spheres is a vanishingly small point, but in practice, because the magnet and ball bearing are imperfect spheres made of non-idealized materials, $r_F > 0$. Lastly, the normal force is minimized by offsetting the magnetic force (F_B) with a counter-weight in such a way that the gravitational force (F_g) is approximately equal to the magnetic force. More specifically, the magnitude of the normal force within a WMB, such as the one shown in figure 2, can be calculated using the following force-balance:

$$F_N = F_B - F_g = F_B - mg \tag{8}$$

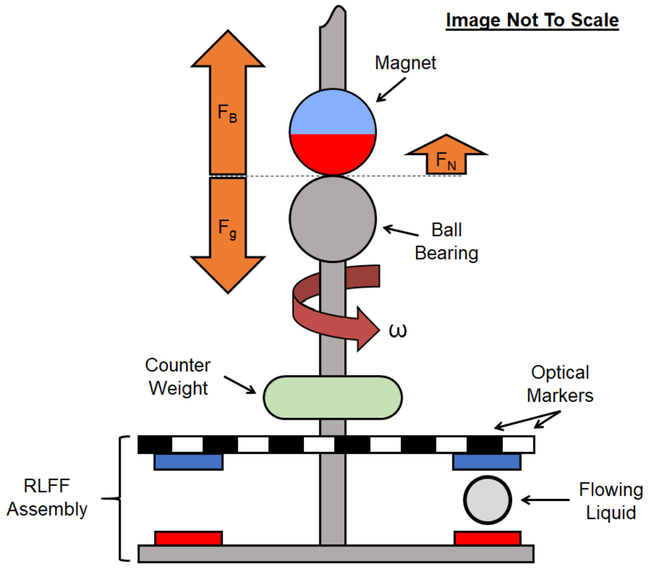

Figure 2. A simple force diagram of showing the operation of a 'WMB'. The ball bearing is made from a magnetic material, such as steel. The small contact area between the magnet and the bearing can be lubricated. The mass of the counter-weight can be adjusted to reduce the magnitude of the normal force between the two spheres. Flow is directed into the page.

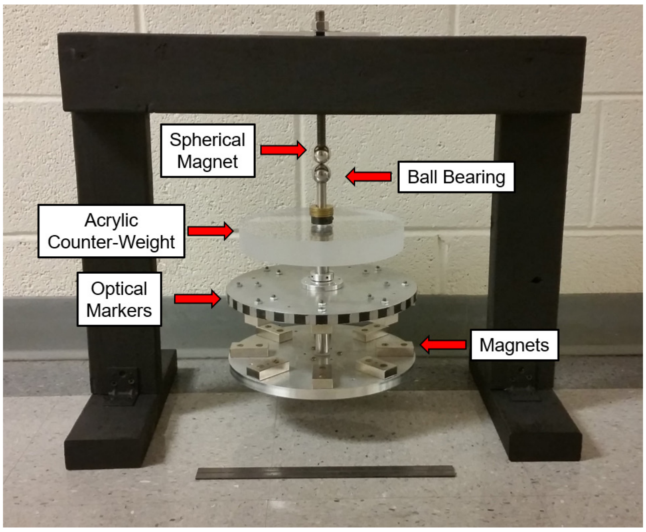

Figure 3. A photo of the RLFF used in this experiment. The spherical magnet remained fixed while the ball bearing and other attached components could rotate about the central axis. Different counterweights could be added or removed to the RLFF to adjust the amount of friction in the bearing. A 1 (ft) ruler is pictured in the foreground for scale.

where m is the combined mass of the RLFF and the counter-weight, and $g \approx 9.81$ (m s^{-2}). For a given magnetic force F_B, the mass of a counter-weight can be increased until the normal force is arbitrarily small ($F_N > 0$ for the bearing to stay connected). The magnitude of F_B for any magnet configuration can be numerically calculated using the techniques described by Meeker [31].

If a WMB is used in a single-sided RLFF, such as those used by Priede *et al* [32] or Bucenieks [18, 22], care should be given to account for electromagnetic lift forces generated by the RLFF [33–35]. These lift forces (F_L) could be problematic during flowmeter startup or flow transients when the relative velocity between the fluid and the magnets is the greatest. Depending on the geometry of the single-sided RLFF, F_L could either increase the normal force and friction between the magnet and the ball bearing or cause the magnet and ball bearing to separate ($F_N = 0$) in very carefully balanced WMBs. As described by Reitz and Davis [36, 37] the ratio of drag force (F_D—see equation (1)) to F_L can be described as

$$\frac{F_D}{F_L} \sim \frac{2}{v_{rel}\sigma\mu_0 D_h}. \tag{9}$$

So, during steady-state operation when $v_{rel} \approx 0$, the lift forces will be minimized.

3.2. Eddy current losses

Due to the design of the WMB used in this experiment, electrically conductive components rotate within a magnetic field. Therefore, it is important to investigate the impact of eddy current losses (P_{EC}) within the bearing. As found in previous work, the eddy current losses can be described as [38–40]

$$P_{EC} \propto \sigma B^2 \omega^2. \tag{10}$$

At low flow rates where the corresponding angular velocity of the RLFF is small, the impact of P_{EC} quickly diminishes. At higher flow rates, the impact of eddy current losses can be reduced by constructing the WMB from materials that have high electrical resistivities. Similarly, rotating components within the magnetic field could be fabricated using thin laminations of magnetic materials to help reduce P_{EC} [41–43]. It is also possible that an electromagnet could be used within the WMB instead of a permanent magnet. In this case, the magnitude of the magnetic field could be adjusted to be as low as possible in order to minimize the effects of the eddy current losses.

3.3. Windage losses

Windage losses (P_W) are due to air resistance on the rotating parts of the RLFF. For simple cylindrical geometries like those found in most RLFFs, it has been shown that P_W scales as [44, 45]

$$P_W \propto D^3 \omega^3. \tag{11}$$

Windage losses could have a substantial impact on RLFF performance at high rotational velocities. One way to reduce the impact of these losses is to design an RLFF to be more aerodynamic, which could be accomplished by eliminating bluff surfaces and keeping the overall size for the RLFF as small as practical. Alternatively, since windage losses become exceedingly small as the angular velocity approaches zero, RLFFs also can be designed to operate under low-flow conditions where the windage losses are negligible.

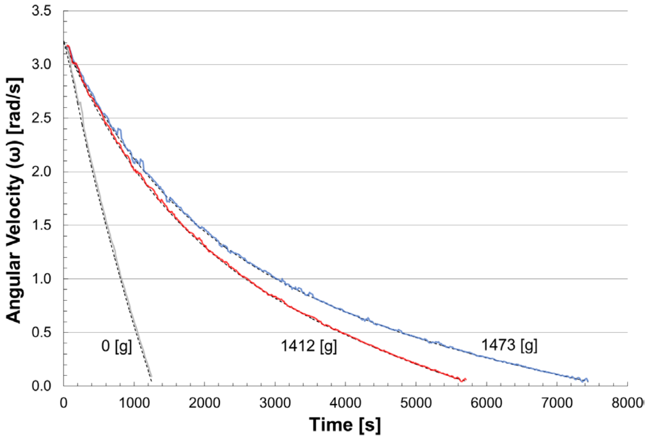

Figure 4. Comparison of the flowmeter deceleration due to bearing and windage losses for different counter-weight masses. The initial angular velocity in each trial was approximately 3.2 (rad s^{-1}). The plotted data is the 5-point moving average of raw data collected every 10 (s). 6th order polynomial fits are overlaid on top of the average data to show the general trend of the RLFF deceleration. Data collection was stopped when less than one optical marker crossed the tachometer in a 10 (s) interval ($\omega_{min} \approx 0.021$ (rad s^{-1})).

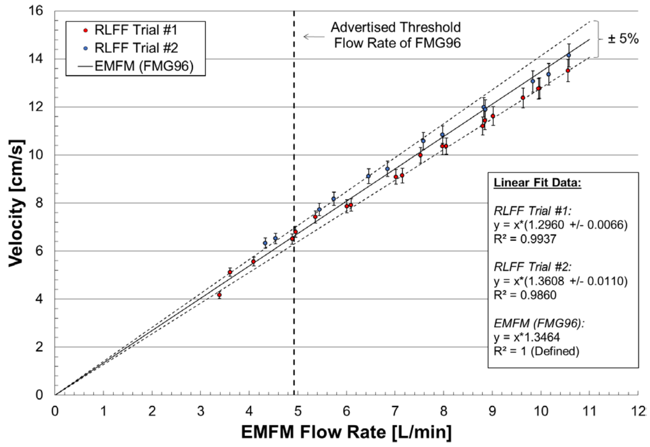

Figure 5. A comparison of the uncalibrated RLFF measurements to the output of the FMG96 electromagnetic flowmeter. The FMG96 had a rated accuracy of 5% over this range of flow rates and has an advertised minimum flow rate of 4.9 (l min^{-1}). The error in the RLFF measurements is about 3.3% for all data points, which corresponded to inaccuracies aligning the RLFF during installation and measuring the effective radius of the device.

4. Experimental setup

The double-sided RLFF used in this experiment was constructed with a WMB, as pictured in figure 3. The RLFF magnet assembly consisted of two aluminum discs ($D = 25.4$ (cm)) each containing eight evenly spaced NdFeB N42 magnets ($5.08 \times 2.54 \times 1.27$ (cm)). The discs were arranged to produce an alternating magnetic field across the fluid. Thirty evenly-spaced optical markers along the rim of the top disc allowed the angular velocity of the disc to be measured with an optical tachometer. The output from the tachometer was collected using a LabVIEW-based data acquisition system. (This configuration closely resembles the RLFF setup used in previous work by this research group [5].)

An AISI 52100 chrome steel ball bearing with a diameter of 2.54 (cm) was attached to the top of the RLFF shaft. The RLFF assembly was then suspended from a spherical, nickel-plated NdFeB magnet with a diameter of 2.54 (cm). Prior to operation, a light coating of WD-40 was applied to the sliding surfaces of the ball bearing and magnet with a lint free cloth. Annular counter-weights were also concentrically fitted onto the central shaft of the RLFF. The counter-weights were designed to be easily accessible so that the total mass of the flowmeter could be adjusted by adding or removing discs. The entire device was supported by a frame that allowed the RLFF to be positioned around the liquid-metal tube. The frame was made from wood in order to avoid interactions with the RLFF magnets (e.g. magnetic attraction, induced eddy currents, etc).

The RLFF design was tested within the Liquid Metal eXperiment Upgrade (LMX-U) at Princeton Plasma Physics Laboratory (PPPL), which has been previously described in other works [46, 47]. LMX-U uses a gear-pump to circulate a liquid metal known as galinstan ($Ga^{67}In^{20.5}Sn^{12.5}$ wt.%) through plastic tubing with an inner diameter of d = 3.97 (cm). The electrical conductivity of galinstan is approximately 3.1×10^6 (S m^{-1}) [48–50]. A commercially available Omega FMG96 electromagnetic flowmeter (EMFM) was used to verify the results of the RLFF. The certified FMG96 was factory calibrated and tested according to NIST standards. This electromagnetic flowmeter has a rated accuracy of ±5% at flow rates of interest to this paper (4.9–12.5 (l min^{-1})) [51].

For this experiment the range of measured average velocities was $v_0 \approx 0.04 - 0.15$ (m s^{-1}) (Re $\approx 4.3E3 - 1.6E4$ [−]). Using equation (3), the turbulent hydrodynamic entrance length was calculated to be a maximum of 15 hydraulic diameters. During testing, the RLFF was installed approximately 18 hydraulic diameters downstream of the pump and all other flow obstructions, so it was assumed that the velocity profile was fully developed during all tests.

5. Results

5.1. Use of counterweights to reduce frictional losses

Frictional losses within the WMB were investigated for different counter-weight masses. As shown in figure 4, increasing the mass of the counter-weight reduced the normal force between the spherical magnet and the ball bearing thereby reducing frictional losses, as predicted by equations (7) and (8). The deceleration curves shown in figure 4 were measured for different counter-weight masses while the RLFF was positioned away from the liquid-metal or any other external conductive or magnetic materials ($\tau_L = 0$).

Without a counter-weight, the RLFF took about 20 (min) to decelerate from an initial angular velocity of approximately

3.2 (rad s^{-1}), which was already a large improvement over previous work [5]. With a 1473 (g) counterweight, the RLFF spun freely for over 120 (min) when given the same initial angular velocity.

5.2. Flowmeter results

The frictionless assumption ($\tau_F = 0$) was tested by comparing uncalibrated RLFF flow rate measurements to the output of the FMG96, as shown in figure 5. The uncalibrated RLFF values were calculated using equation (5), where the effective radius ($r \approx 9.84$ (cm)) was assumed to be the distance from the RLFF axis of rotation to the center of the pipe. It was determined that the uncertainty in the RLFF measurements was about 3.3%, which primarily resulted from errors in measuring the effective radius since ω was very accurately known. This error corresponds to the effective radius being known to within approximately ± 1.5 (mm). The average flow velocity of the galinstan was also calculated using the volumetric flow rate (Q) data measured by the EMFM and the following relation:

$$v_0 = \frac{4\,Q}{\pi d^2}. \qquad (12)$$

Figure 5 shows that the uncalibrated results from the RLFF fall within the $\pm$ 5% uncertainty margin of the EMFM. The RLFF was tested on two separate dates by two different operators. The device was removed and reinstalled around the liquid-metal filled pipe between each trail. Due to the RLFF not being installed in the exact same position during each test, small differences in the two data sets are expected.

It is also noteworthy that the RLFF was capable of generating steady outputs at flow rates lower than what the EMFM could measure. During the experiment the gear pump could operate smoothly at speeds as low as 50 (RPM). Assuming there was no fluid slipping past the gears in the pump, which experiments have shown to be an overly optimistic assumption, the maximum expected output of the pump would be $\approx$2.50 (l $\min^{-1}$) or $\approx$3.37 (cm s^{-1}) [52]. Under these conditions the RLFF rotated at $\omega \approx 0.33$ (rad s^{-1}) which corresponded to a flow rate of $\approx$3.06 (cm s^{-1}). This is a promising and encouraging result because it is close to but less than the maximum expected output of the gear pump. Based on these results, operational experience with the RLFF, and the deceleration curves in figure 4, it is extremely likely that the RLFF would be able to measure even smaller flow rates if it were tested with different experimental hardware.

6. Discussion and future work

A novel RLFF was designed, built, and tested. The performance of the WMB was adjusted by changing the mass of a counter-weight in order to reduce the normal force between the spherical magnet and the steel ball bearing. For carefully selected counter-weight masses, it was shown that a WMB can nearly eliminate frictional losses in an RLFF.

The advantages of using a WMB to minimize frictional losses in an RLFF are two-fold:

- The RLFF can be used without calibration and still achieve accuracies comparable to commercially available flowmeters.
- The RLFF has improved sensitivity at low flow rates when compared to using traditional roller bearings [5]. (For this experiment, the RLFF could measure flow rates that were too small for the commercially available flowmeter used to verify RLFF operation.)

These improvements have the potential to make RLFFs better suited to industrial applications where easy, precise, and accurate measurements of flows are required. However, it should be emphasized that not all loss mechanisms within the RLFF were reduced (see section 3). At large RLFF angular velocities, windage or eddy current losses could become appreciable and require the device to be calibrated. Furthermore, it should be reiterated that the fluid in this experiment flowed through non-magnetic, electrically-insulating plastic tubing. The use of metal pipes or tubes would have likely affected the output of the RLFF [3, 18, 22].

Work on RLFFs will continue at Princeton University with a focus on the following areas:

- The development of lighter components to improve the transient performance and response time of the flowmeter.
- Better techniques to install and align the RLFF with the liquid-metal filled tube. More accurate and consistent positioning of the flowmeter around the pipe would reduce uncertainty in the measurements.
- Streamlining the RLFF magnet assembly in order to reduce windage losses and allow for more accurate measurements at higher flow rates.

Acknowledgments

The research described in this paper was conducted under the Laboratory Directed Research and Development Program (LDRD) at Princeton Plasma Physics Laboratory, a national laboratory operated by Princeton University for the US Department of Energy under Prime Contract Number DE-AC02-09CH11466.

The digital data for this paper can be found at http://arks.princeton.edu/ark:/88435/dsp01x920g025r

Appendix

A.1. Nomenclature

Variable	Meaning	Units
b	Induced magnetic field	T
B	External magnetic field	T
d	Inner diameter of pipe or tube	m
D	Diameter of RLFF disc	m
D_h	Hydraulic diameter	m
F	Force	N
g	Gravitational acceleration	m s^{-2}
I	Moment of inertia	kg m^{-2}
K_L	Lorentz factor	N s
L	Hydrodynamic entrance length	m
m	Mass	kg
N	Interaction parameter	—
P	Power loss	W
Q	Volumetric flow rate	m^3 s^{-1}
r	Radius	m
Re	Reynolds #	—
Re_m	Magnetic Reynolds #	—
v_0	Average fluid velocity	m s^{-1}
v_{mag}	Average magnet velocity	m s^{-1}
v_{rel}	Relative velocity	m s^{-1}
α	Angular acceleration	rad s^{-2}
μ	Viscosity	Pa-s
μ_0	Vacuum permeability	H m^{-1}
μ_K	Coefficient of kinetic friction	—
ρ	Density	kg/m^3
σ	Electrical conductivity	S m^{-1}
τ	Torque	N m
ω	Angular velocity	rad s^{-1}
Abbreviation	Meaning	
EMFM	Electromagnetic flowmeter	
LMX-U	Liquid Metal eXperiment—Upgrade	
PPPL	Princeton Plasma Physics Laboratory	
RLFF	Rotating Lorentz-force flowmeter	
WMB	Weighted magnetic bearing	
Mathematical convention	Meaning	
$A(x)$	'A' is a function of 'x'	

ORCID iDs

M G Hvasta https://orcid.org/0000-0002-8934-711X
D Dudt https://orcid.org/0000-0002-4557-3529
A E Fisher https://orcid.org/0000-0003-1744-6984
E Kolemen https://orcid.org/0000-0003-4212-3247

References

[1] Shercliff J A 1957 Tests with mercury of a rotary flowmeter for liquid metals *A.E.R.E. X/M 169* United Kingdom Atomic Energy Authority
[2] Shercliff A J 1960 Improvements in or relating to electromagnetic flowmeters *GB Patent* GB831226
[3] Shercliff J A 1962 *The Theory of Electromagnetic Flow-Measurement* (Cambridge: Cambridge University Press)
[4] Thess A, Votyakov E V and Kolesnikov Y 2006 Lorentz force velocimetry *Phys. Rev. Lett.* **96** 164501
[5] Hvasta M G, Slighton N T, Kolemen E and Fisher A E 2017 Experimental calibration procedures for rotating Lorentz-force flowmeters *Meas. Sci. Technol.* **28** 085901
[6] Priede J, Buchenau D and Gerberth G 2009 Force-free and contactless sensor for electromagnetic flowrate measurements *Magnetohydrodynamics* **45** 451–8
[7] Eckert S, Buchenau D, Gerbeth G, Stefani F and Weiss F P 2011 Some recent developments in the field of measuring techniques and instrumentation for liquid metal flows *Nucl. Sci. Technol.* **48** 490–8
[8] Ebert R, Leineweber J and Resagk C 2015 Performance enhancement of a Lorentz force velocimeter using a buoyancy-compensated magnet system *Meas. Sci. Technol.* **26** 075301
[9] Halbedel B, Resagk C, Wegfrass A, Diethold C, Werner M, Hilbrunner F and Thess A 2014 A novel contactless flow rate measurement device for weakly conducting fluids based on Lorentz force velocimetry *Flow Turbul. Combust.* **92** 361–9
[10] Wegfrass A, Diethold C, Werner M, Frohlich T, Halbedel B, Hilbrunner F, Resagk C and Thess A 2012 A universal noncontact flowmeter for liquids *Appl. Phys. Lett.* **100** 194103
[11] Wiederhold A, Ebert R, Weidner M, Halbedel B, Frohlich T and Resagk C 2016 Influece of the flow profile to Lorentz force velocimetry for weakly conducting fluids—an experimental validation *Meas. Sci. Technol.* **27** 125306
[12] Buchenau D, Galindo V and Eckert S 2014 The magnetic flywheel flow meter: theoretical and experimental contributions *Appl. Phys. Lett.* **104** 223504
[13] Wang X, Kolesnikov Y and Thess A 2012 Numerical calibration of a Lorentz force flowmeter *Meas. Sci. Technol.* **23** 045005
[14] Alferenok A, Potherat A and Luedtke U 2013 Optimal magnet configurations for Lorentz force velocimetry in low conductivity fluids *Meas. Sci. Technol.* **24** 065303
[15] Minchenya V, Karcher C, Kolesnikov Y and Thess A 2011 Calibration of the Lorentz force flowmeter *Flow Meas. Instrum.* **22** 242–7
[16] Kolesnikov Y, Karcher C and Thess A 2001 Lorentz Force flowmeter for liquid aluminum: laboratory experiments and plant tests *Metall. Mater. Trans.* B **42B** 441
[17] Heinicke C 2013 Spatially resolved measurements in a liquid metal flow with Lorentz force velocimetry *Exp. Fluids* **54** 1560
[18] Bucenieks I 2014 Modelling of induction rotary permanent magnet flowmeters for liquid metal flow control *Magnetohydrodynamics* **50** 157–64
[19] Thess A, Votyakov E, Knaepen B and Zikanov O 2007 Theory of the Lorentz force flowmeter *New J. Phys.* **9** 1–27
[20] Roberts P H 1967 *An Introduction to Magnetohydrodynamics* (New York: American Elsevier)
[21] Vire A, Knaepen B and Thess A 2010 Lorentz force velocimetry based on time-of-flight measurements *Phys. Fluids* **22** 125101
[22] Bucenieks I 2007 Experimental measurements of sensitivity of cylindrical rotary induction flowmeter on permanent magnets *2nd Int. Workshop on Measuring Techniques for Liquid Metal Flows (MTLM 2007) (Dresden)*
[23] Rosemount Measurement 1995 *Magnetic Flowmeter Fundamentals* (*TDS 3032A00*) https://www.automaatika.ee/pdf/Fundament.pdf (Rosemount Measurement)
[24] National Measurement System 2010 *Good Practice Guide: An Introduction to Flow Meter Installation Effects* (TUV NEL)

[25] Livelli G 2010 Flowmeter piping requirements Flow Control Network (Online) www.flowcontrolnetwork.com/flowmeter-piping-requirements/ (Accessed: April 2018)
[26] Cengel Y A and Cimbala J M 2006 *Fluid Mechanics: Fundamentals and Applications* 1st edn (New York: McGraw-Hill)
[27] Bhatti M S and Shah R K 1987 Turbulent and transition flow convective heat transfer in ducts *Handbook of Single-Phase Convective Heat Transfer* ed S Kakac *et al* (New York: Wiley)
[28] Marion J B and Hornyak W F 1982 *Physics for Science and Engineering (Part 1)* (Philadelphia, PA: Saunders)
[29] Sears F W, Zemansky M W and Young H D 1988 *University Physics* 7th edn (Reading, MA: Addison-Wesley)
[30] Van Name F W Jr 1958 *Analytical Mechanics* (Engelwood Cliffs, NJ: Prentice-Hall)
[31] Meeker D 2015 *Finite Element Method Magnetics Version 4.2 User's Manual* http://www.femm.info/Archives/doc/manual42.pdf
[32] Priede J, Buchenau D and Gerbeth G 2011 Single-magnet rotary flowmeter for liquid metals *J. Appl. Phys.* **110** 034512
[33] Jayawant B V 1981 Electromagnetic suspension and levitation *Rep. Prog. Phys.* **44** 411
[34] Jayawant B V 1982 Electromagnetic suspension and levitation *IEE Proc.* A 549–81
[35] Fujii N, Ogawa K and Matsumoto T 1996 Revolving magnet wheels with permanent magnets *Electr. Eng. Japan* **116** 319–26
[36] Reitz J R and Davis L C 1972 Force on a rectangular coil moving above a conducting slab *J. Appl. Phys.* **43** 1547
[37] Davis L C and Reitz J R 1971 Eddy currents in finite conducting sheets *J. Appl. Phys.* **42** 4119
[38] Schafer R and Heiden C 1976 Eddy current losses of cylindrical conductors rotating in a magnetic field *Appl. Phys.* **9** 121–5
[39] Fiorillo F 2004 *Measurement and Characterization of Magnetic Materials* (New York: Elsevier)
[40] Aubert G, Jacquinot J F and Sakellariou D 2012 Eddy current effects in plan and hollow cylinders spinning inside homogeneous magnet fields: application to magnetic resonance *J. Chem. Phys.* **137** 154201
[41] Barranger J 1965 Hysteresis and eddy-current losses of a transformer lamination viewed as an application of the poynting theorem (Cleveland, OH: National Aeronautics and Space Administration (NASA))
[42] Paulides J J H, Meessen K J and Lomonova E A 2008 Eddy-current losses in laminated and solid steel stator back iron in a small rotary brushless permanent-magnet actuator *IEEE Trans. Magn.* **44** 4373–6
[43] Appleyard R E and Ringland W L 1969 Alternating-current generators *Standard Handbook for Electrical Engineers* 10th edn, ed D G Fink and J M Carroll (New York: McGraw-Hill) p 9
[44] Vrancik J E 1968 Prediction of windage power loss in alternators *NASA TN D-4849* (Cleveland: Lewis Research Center)
[45] Raymond M S, Kasarda M E F and Allaire P E 2008 Windage power loss modeling of a smooth rotor supported by homopolar active magnetic bearings *J. Tribol.* **130** 021101
[46] Hvasta M G, Kolemen E and Fisher A E 2017 Application of IR imaging for free-surface velocity measurements in liquid-metal systems *Rev. Sci. Instrum.* **88** 013501
[47] Hvasta M G, Kolemen E, Fisher A E and Ji H 2017 Demonstrating electromagnetic control of free-surface, liquid-metal flows relevant to fusion reactors *Nucl. Fusion* **58** 016022
[48] Nornberg M D, Ji H, Peterson J L and Rhoads J R 2008 A liquid metal flume for free surface magnetohydrodynamic experiments *Rev. Sci. Instrum.* **79** 094501
[49] Morley N B, Burris J, Cadwallader L C and Nornberg M D 2008 GaInSn usage in research laboratory *Rev. Sci. Instrum.* **79** 056107
[50] Plevachuk Y, Skylarchuk V, Eckert S, Gerbeth G and Novakovic R 2014 Thermophysical properties of the liquid Ga–In–Sn eutectic alloy *J. Chem. Eng. Data* **59** 757–63
[51] Omega 2015 FMG90 Series Electromagnetic Flow Meter User's Guide www.omega.com/manuals/manualpdf/M5204.pdf
[52] Oberdorfer Pumps Chemsteel Series S930 Metallic *Manual* (Oberdorfer Pumps)